TUTORIAL / ARTICLE DIDACTIQUE

A home-built lock-in amplifier for laser frequency stabilization

K. Sowka, M. Weel, S. Cauchi, L. Cockins, and A. Kumarakrishnan

Abstract: We describe an inexpensive lock-in amplifier that can be built using discrete off-the-shelf RF components and home-built analog circuits. This lock-in has been used in a feedback loop to lock the frequency of a laser to an atomic transition. The frequency stability was tested by trapping rubidium atoms. The feedback loop involves obtaining a modulated saturated absorption signal from a vapor cell using an acousto-optic modulator to modulate the laser frequency. The absorption signal is sent to the lock-in to generate an error signal, proportional to the first derivative of the absorption, which is fed back to the laser to complete the feedback loop. We also demonstrate a simplified optical setup for viewing the saturated absorption spectrum. In this case, the signal consists of narrow saturated absorption spectra riding on top of a Doppler-broadened pedestal. We show that it is possible to greatly reduce the effect of this background and lock the laser to the atomic resonance by modifying the home-built lock-in to generate an error signal proportional to the third derivative of the absorption. The results of this work can be adapted for advanced undergraduate laboratory work.

PACS Nos.: 01.50Pa, 07.50.−e, 42.62Fi, 42.60Fc

Résumé : Nous décrivons ici un amplificateur synchrone à faible coût que l'on peut construire en utilisant des composantes RF couramment disponibles et des circuits analogues faits maison. Nous avons utilisé cet amplificateur dans une boucle de rétroaction pour fixer la fréquence d'un laser sur celle d'une transition atomique. Nous avons vérifié la stabilité de la fréquence en piégeant des atomes de rubidium. La boucle de rétroaction requiert l'obtention d'un signal d'absorption saturé modulé de la cellule contenant la vapeur en utilisant un modulateur acousto-optique (AOM) pour moduler la fréquence du laser. Le signal d'absorption est envoyé à l'amplificateur synchrone pour générer un signal d'erreur proportionnel à la première dérivée de l'absorption, qui est ensuite envoyé au laser pour compléter la boucle de rétroaction. Nous proposona également un montage optique simplifié pour observer le spectre d'absorption saturé. Dans ce cas, le signal consiste en un étroit

K. Sowka, M. Weel, S. Cauchi, L. Cockins, and A. Kumarakrishnan.[1] Department of Physics, York University, 4700 Keele St., Toronto, ON M3J 1P3, Canada.

[1]Corresponding author (e-mail: akumar@yorku.ca).

spectre d'absorption saturé chevauchant une base élargie Doppler. Nous montrons qu'il est possible de réduire de façon importante ce signal de fond et de synchroniser le laser sur la résonance atomique en modifiant l'amplificateur synchrone maison pour générer un signal d'erreur proportionnel à la troisième dérivée de l'absorption. Les résultats de ce travail peuvent être adaptés à des laboratoires avancés pour étudiants de premier cycle.

[Traduit par la Rédaction]

1. Introduction

Lasers with a broad-gain profile can be made tunable by using wavelength-selecting elements, such as gratings and etalons, that restrict the laser emission to a narrow frequency interval. Typically, the cavity length of the laser is controlled by sending a DC voltage to a piezo-electric transducer attached to one or more of the optical elements associated with the laser cavity. This permits the laser frequency to be tuned continuously across the gain profile. However, the sensitivity of the tuning parameters to additional factors such as current, temperature, or mechanical fluctuations causes the central frequency of the laser to drift. Consequently, applications in laser spectroscopy such as laser cooling and trapping of neutral atoms require active frequency stabilization. The standard method involves generating a DC error signal, with a zero-crossing at the lock point, to be used in a feedback loop that continuously corrects the laser frequency.

Lock-in amplifiers are widely used for frequency-stabilization techniques. For this application, generating the error signal requires imposing a small modulation on the laser frequency [1] and passing a beam through a vapor cell containing a dilute atomic vapor. The atomic spectra provide a frequency reference. The modulated laser frequency is scanned over an atomic resonance so that a modulated absorption signal can be recorded. This signal is sent to the lock-in where it is mixed with the original modulation to produce a DC error signal proportional to the first derivative of the absorption. This line shape is suitable for correcting the frequency since it contains a sloping section crossing zero at the resonant frequency. After the amplitude and filtering parameters of the error signal are adjusted, the scan is turned off and the feedback loop engaged. Figure 1 shows the main elements of the loop.

Extensive mathematical descriptions of the lock-in techniques and properties of line shapes used for locking have been described previously [2, 3]. However, to explain lock-in techniques for advanced undergraduate laboratories it is instructive to develop a physical explanation and a simple mathematical model for the shape of the feedback signal [4]. We have implemented this technique using a commercial lock-in amplifier to lock lasers used in atom-trapping experiments for time scales of the order of 1 h. Although the method is simple and robust, the laser beam going to the experiment is frequency modulated thereby causing residual heating of the cold sample. This can be avoided by sending the modulation to an electro-optic phase modulator (EOM) [5] or an acousto-optic modulator (AOM) [6] placed in front of the reference cell. In our experiments, we used an AOM operating in the Bragg regime, to frequency shift the laser beam. The AOM was driven by a voltage-controlled, frequency-modulated oscillator (VCO) so that the central frequency of the AOM can be modulated. Although the frequency modulation causes the diffracted beam to be deflected back and forth, this effect can be eliminated by operating the AOM in a dual pass configuration [7] as shown in Fig. 2. This technique is widely used in laser spectroscopy. An additional advantage of using an AOM is that the stabilized laser frequency can be shifted simply by changing the central frequency of the AOM.

In this paper we show that an inexpensive lock-in amplifier can be constructed using discrete off-the-shelf RF components and home-built analog circuits. This device is versatile and can replicate expensive options available in commercial lock-ins, such as the display of the in phase and quadrature components of the error signal as well as offering the flexibility to generate higher order derivatives of absorption signal.

For applications related to atom trapping, it is necessary to stabilize the laser frequency to within ~1 MHz of the desired atomic resonance. Since the Doppler width of the atomic vapor in the vapor cell

Fig. 1. Overall setup for frequency stabilization using a lock-in amplifier: The absorption and error signals shown are produced when the laser frequency is scanned over the atomic resonance; the scan is turned off before engaging feedback.
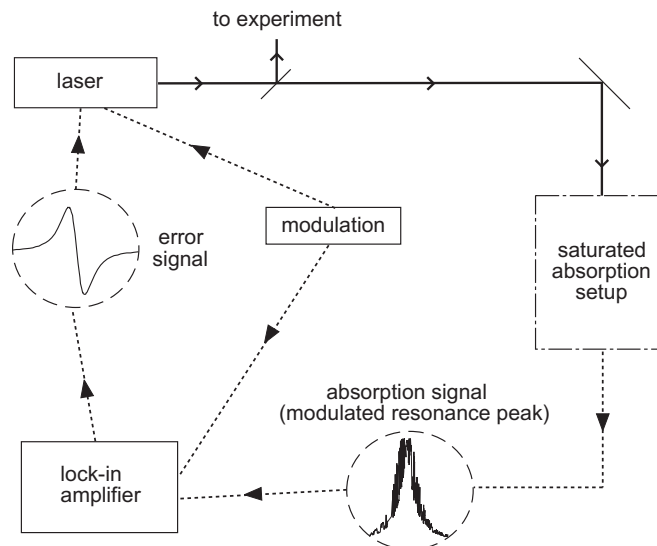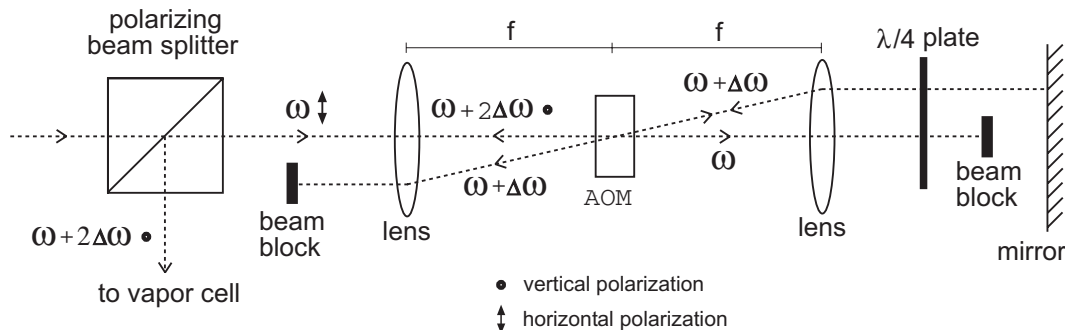

Fig. 2. Dual-pass AOM: The incoming and outgoing beams have orthogonal polarizations. The AOM is used to frequency modulate the laser beam going to the Rb vapor cell. It also serves to frequency shift the stabilized laser beam used for atom trapping.
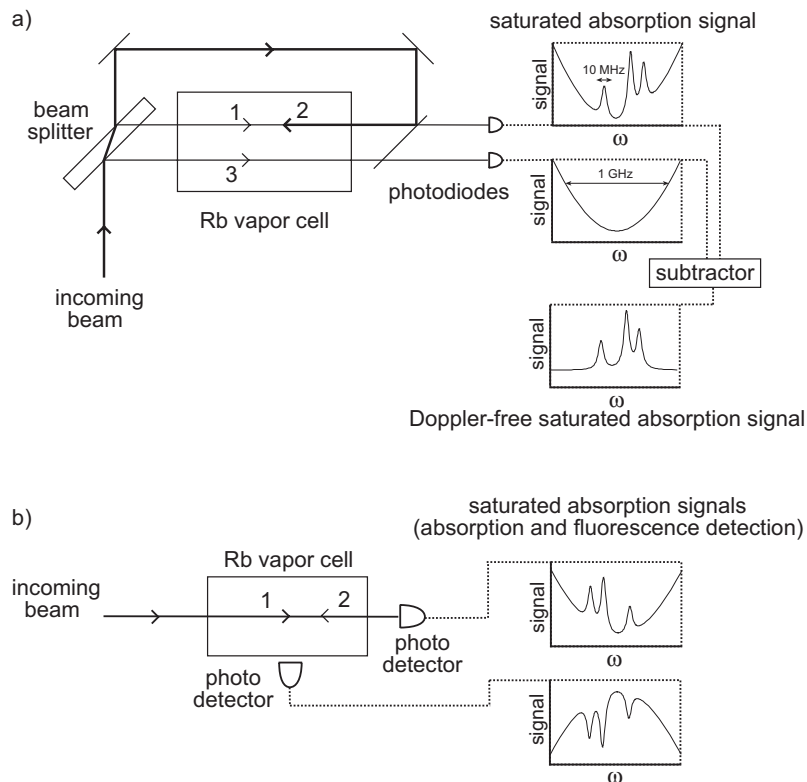

is ~1 GHz it is necessary to generate a narrow resonance to which the laser frequency can be locked. Figure 3*a* illustrates the standard technique (saturated absorption spectroscopy) for generating a narrow resonance.

A weak (i.e., $I \ll I_{sat}$) probe beam (1) and a counter propagating intense (i.e., $I \sim I_{sat}$) pump beam (2), derived from the same laser, are directed through the vapor cell. Here, I_{sat} is the saturation intensity of the atomic transition. In the presence of the pump beam, the absorption of the probe beam is reduced for a narrow velocity class centered at zero velocity. As a result, when the laser is scanned, narrow spectral features (Lamb dips) are recorded at resonant frequencies in the Doppler-broadened absorption profile of the probe laser. The widths of the Lamb dips are of the order of the power-broadened natural line width for the atomic transitions (~10 MHz). Another weak reference beam (3) passing through the vapor cell is used to record the Doppler background during the same scan. The Doppler-free resonance peak is observed by electronically subtracting the Doppler-broadened line shape from the saturated absorption signal. The first derivative of this signal can be used as feedback to lock to a resonance peak.

We demonstrate a simpler technique for viewing the saturated absorption spectrum, shown in Fig. 3*b*.

Fig. 3. (*a*) standard setup for obtaining a Doppler-free saturated absorption signal: (1) weak probe beam, (2) counter-propagating intense pump beam, (3) weak reference beam, (*b*) simplified setup for obtaining the saturated absorption signal: The signal can be be observed by absorption or fluorescence detection.

a)   saturated absorption signal

beam splitter

1   2

3

Rb vapor cell

photodiodes

10 MHz

1 GHz

subtractor

incoming beam

Doppler-free saturated absorption signal

b)   saturated absorption signals (absorption and fluorescence detection)

Rb vapor cell

incoming beam

1   2

photo detector

photo detector

This method involves generating the counter-propagating beams by retro reflecting the original beam from the window of the vapor cell and detecting the signal through fluorescence or absorption. The first derivative of this signal is unsuitable for locking to a resonant frequency since the Doppler background causes a shift in the position of the observed resonance peaks. However, the effect of the background can be nearly eliminated if, instead of the first derivative, the third derivative of the saturated absorption signal is used as feedback. The third derivative is obtained by mixing the signal using the third harmonic of the modulation frequency [1].

The rest of the paper is organized as follows. In Sect. 2, we model the shape of the first-derivative error signal. For the setup shown in Fig. 3*b*, we represent the shape of the saturated absorption signal as the sum of a Lorentzian (Doppler-free component) and a Gaussian (Doppler-broadened component). We show how the third derivative of the signal can be obtained by mixing it with the third harmonic of the modulation frequency and explain how this process greatly reduces the effect of the Doppler component. Section 3 describes the experimental setup and gives details of simple analog circuits used in the lock-in amplifier. Section 4 shows the first- and third-derivative error signals obtained using the home built lock-in and describes tests that show that the frequency stability is comparable to the performance of a commercial device.

2. Theory

We now explain the basic features of the error signal. When the frequency-modulated laser is scanned over the desired Doppler-free resonance at ω_0, the modulated absorption signal is recorded by a photo detector and sent to the lock-in amplifier. The lock-in multiplies this signal with the phase-shifted

modulation signal. It then filters out the AC components to generate the error signal. The error signal is positive above resonance, negative below resonance, and zero on resonance. A physical explanation for the shape of the error signal produced by a lock-in and a simple mathematical model are given in ref. 4.

We now describe an alternate method for explaining the shape of the error signal. This method shows explicitly that the error signal is proportional to the first derivative of the absorption signal and that higher order derivatives can be obtained by mixing the absorption signal with higher harmonics of the modulation frequency. Assuming that the drifts of the central laser frequency ω_c are slow compared to the period of the frequency modulation, the time-dependent expression for the modulated laser frequency ω_L can be written as

$$\omega_L = \omega_c + A\cos(\Omega t) \tag{1}$$

The amplitude and frequency of the modulation are represented by A and Ω, respectively. The Doppler-free absorption signal $S_1(\omega_L)$ consisting of a resonance peak at ω_0 can be represented by a Lorentzian line shape given as

$$S_1(\omega_L) = L(\omega_L) = \frac{\alpha}{\beta + [\omega_L - \omega_0]^2} \tag{2}$$

The constants α and β are shape parameters that control the amplitude and width of the Lorentzian, respectively. Restricting the amplitude of the frequency modulation A to be small enough such that the absorption signal containing the Lorentzian line shape can be approximated by a first-order Taylor expansion in ω_L about ω_c.

$$S_1(\omega_L) \simeq L(\omega_c) + L'(\omega_c)[\omega_L - \omega_c] = L(\omega_c) + L'(\omega_c)A\cos(\Omega t) \tag{3}$$

The mixer output $M(\omega_L)$ is the product of the absorption signal S_1 and the phase-shifted modulation signal $B\cos(\Omega t + \phi)$. The phase difference between the two signals is written as ϕ and B is the amplitude of the modulation signal.

$$M(\omega_L) \simeq \left[L(\omega_c) + L'(\omega_c)A\cos(\Omega t)\right]\left[B\cos(\Omega t + \phi)\right] \tag{4a}$$

$$M(\omega_L) \simeq L(\omega_c)B\cos(\Omega t + \phi) + \frac{1}{2}L'(\omega_c)AB\cos(2\Omega t + \phi) + \frac{1}{2}L'(\omega_c)AB\cos(\phi) \tag{4b}$$

Equation 4*a* was expanded and simplified using the trigonometric identity $\cos(x)\cos(y) = \frac{1}{2}(\cos(x+y) + \cos(x-y))$ to give (4*b*).

Putting this signal through a low-pass filter ensures that all oscillatory terms are eliminated so that only the last term remains. This term constitutes the first-derivative error signal $E_1(\omega_L)$ shown below.

$$E_1(\omega_L) \simeq \frac{1}{2}L'(\omega_c)AB\cos(\phi) \tag{5}$$

The shape of this error signal is proportional to the first derivative of the absorption signal at ω_c and is explicitly a function of the phase shift ϕ. By controlling ϕ, the amplitude and sign of the error signal can be varied.

In general, it can be shown that signals proportional to higher order derivatives of the absorption can be obtained by mixing the absorption signal with higher harmonics of the modulation frequency. This can be useful for several interesting applications.

As an example, the saturated absorption signal S_2 (see Fig. 3*b*) consists of a narrow Lorentzian line shape (2) riding on a Doppler-broadened background. This background is described by a Gaussian represented by

$$G(\omega_L) = -\gamma \exp\left[-\lambda(\omega_L - \omega_0)^2\right] \tag{6}$$

Fig. 4. (*a*) Relative sizes of the narrow resonance L (broken line) given by (2), the Doppler background G (thin line) given by (6) and the saturated absorption signal S_2 (bold line) modeled as $S_2 = L + G$. (*b*) First derivatives of L, G, and S_2. (*c*) Third derivatives: Compared to the other functions, the third derivative of G is so small that it does not appear on the graph. Consequently, the third derivatives of L and S_2 overlap.
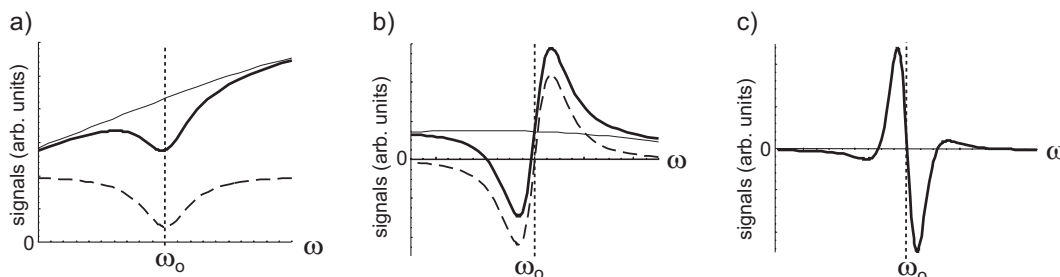
The constants γ and λ are shape parameters that control the amplitude and width of the Gaussian, respectively. The saturated absorption signal S_2 can, therefore, be modeled as

$$S_2(\omega_L) = L(\omega_L) - G(\omega_L) \tag{7}$$

If the first derivative of the saturated absorption signal is used as feedback, the background component of the signal would cause the zero crossing to be shifted to a frequency different from ω_0. However, since the background is approximately linear in the vicinity of the resonance, it can be greatly reduced by taking the third derivative of the signal, as illustrated in Fig. 4. The third derivative of a resonance peak resembles the first derivative and, therefore, is also suitable for locking.

We now show how the third-derivative error signal is obtained by mixing the absorption with the third harmonic of the modulation and filtering out the AC components. The signal given by (7) is written as a third-order Taylor expansion about ω_c, shown below.

$$S_2(\omega_L) \simeq [G(\omega_c) - L(\omega_c)] + A\cos(\Omega t)[G(\omega_c) - L(\omega_c)]' + \frac{1}{2}A^2\cos^2(\Omega t)[G(\omega_c) - L(\omega_c)]''$$

$$+ \frac{1}{6}A^3\cos^3(\Omega t)[G(\omega_c) - L(\omega_c)]''' \tag{8}$$

The mixer output is modeled as the product $S_2(\omega_L)[B\cos(3\Omega t + \phi)]$, where B and ϕ are the amplitude and phase of the third-harmonic modulation signal, respectively. The constant terms of the expanded mixer output become the error signal $E_3(\omega_L)$. Again, using the trigonometric identity $\cos(x)\cos(y) = \frac{1}{2}[\cos(x + y) + \cos(x - y)]$, it is clear that the error signal will be proportional only to terms in S_2 with the factor $\cos(3\Omega t)$. S_2 contains a sum of terms containing nth derivatives of the saturated absorption signal multiplied by $\cos^n(\Omega t)$. However, $\cos^n(\Omega t)$ can be expanded, using known trigonometric identities, as a linear function of cos terms with angular frequencies n, $n - 2$, ... ≥ 0. Consequently, it can be shown that the error signal $E_3(\omega_L)$, shown below, is proportional to the third derivative of the absorption signal at ω_c.

$$E_3(\omega_L) \simeq \frac{1}{48}A^3 B\cos(\phi)[G(\omega_c) - L(\omega_c)]''' \tag{9}$$

As discussed, both the first- and third-derivative error signals are suitable for locking the laser frequency to the peak of an atomic resonance. Although the third-derivative signal has a lower signal-to-noise ratio, it automatically reduces the effect of a Doppler background. Additionally, since the width of the signal close to resonance and between the turning points is narrower than for the case of the first derivative it can be used to obtain a more precise lock. However, this results in a smaller recapture range for correcting the laser frequency.

Fig. 5. Our experimental setup for obtaining the first-derivative error signal.
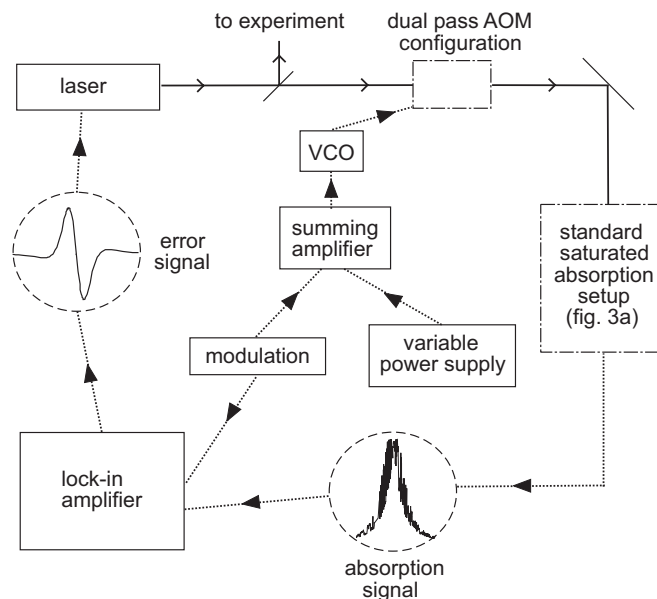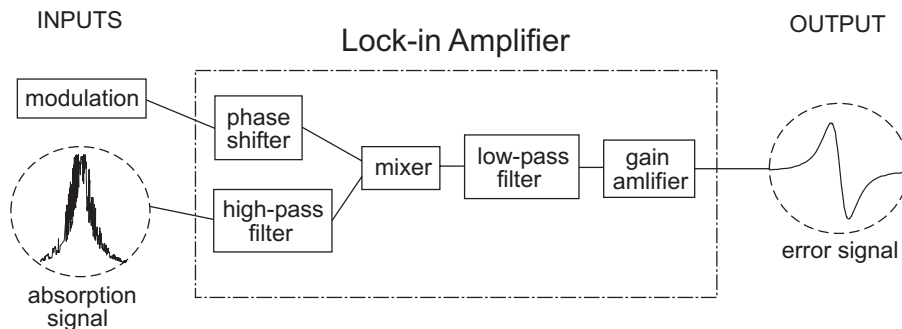

Fig. 6. Schematic diagram of lock-in amplifier.

3. Experimental setup

The modulation frequency should be chosen so that it does not correspond to the frequencies of local sources of noise that may include room lights, pumps, and RF sources. For our experimental setup shown in Fig. 5, the modulation frequency Ω is 50 kHz. The modulation signal is split so that it can be sent to the lock-in and also added to a DC signal used to control the oscillator (VCO) driving the AOM. The amplitude of the frequency modulation for obtaining the first- and third-derivative error signals is $\sim$1 MHz. The inputs to the lock-in amplifier are the saturated absorption signal and the modulation, as shown in Fig. 6. Figure 6 also shows the key elements of the lock-in, which are a phase shifter, a RF mixer, and a low-pass filter. A gain amplifier is added to control the amplitude of the error signal produced. The phase shifter, low-pass filter, and gain amplifier can be built using analog electronics.

The phase shifter, shown in Fig. 7, imposes a phase difference between the modulation signal used for mixing and the modulated absorption signal. The operational amplifier equalizes the voltage inputs V_+ and V_-. Since $V_+ = V_{in} \frac{i\Omega CR}{1+i\Omega CR}$ and $V_- = \frac{V_{in}+V_{out}}{2}$ it is easy to show that the ratio of input and output voltages is given by the complex quantity $\frac{V_{in}}{V_{out}} = -[\frac{1-i\Omega CR}{1+i\Omega CR}]$. The phase shift ϕ is the argument of

Fig. 7. Diagram of phase-shifting circuit.
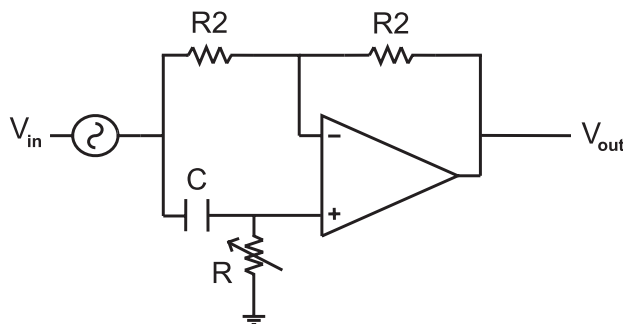
Fig. 8. Circuit diagrams: (*a*) voltage follower, (*b*) low-pass filter, and (*c*) gain amplifier.
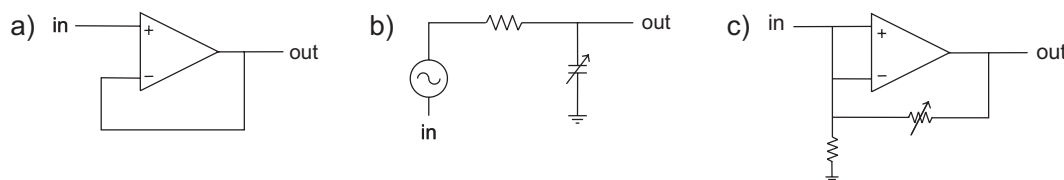
Fig. 9. Experimental setup for obtaining the third harmonic of modulation signal.
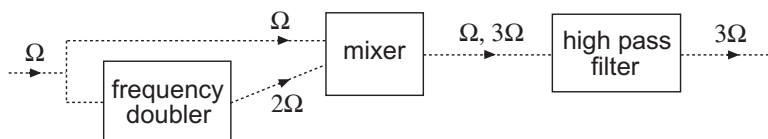
the former complex quantity and is given by $\tan(\phi) = \frac{-2\Omega CR}{1-[\Omega CR]^2}$. Using the identity $\tan(2\alpha) = \frac{2\tan\alpha}{1-\tan^2\alpha}$, it can be shown that $\phi = -2\tan^{-1}\Omega CR$. A variable resistor is used to control the phase difference. Since the maximum phase shift that can be achieved is π, we use two phase shifters in series to get the desired range of 0 to 2π. A voltage follower (Fig. 8*a*) is included before the phase shifters to serve as a buffer. Since this arrangement is easy to modify, it is possible to assemble additional phase shifters for display of the in-phase and quadrature components of the error signal.

The absorption signal and the phase-shifted modulation are multiplied using a commercially available double-balanced RF mixer. Since the DC component of the absorption signal lowers the output of the mixer, it is preferable to high-pass filter the absorption signal before sending it to the mixer. Filtering out the DC component is equivalent to eliminating the first term in the Taylor expansion (see (3) and (8)). This does not affect the error signal since this term would be filtered out in any case, after mixing.

The output of the mixer is sent to a low-pass filter (Fig. 8*b*), with cutoff frequency less than Ω, to eliminate the AC components and produce the error signal. This signal is sent to a voltage amplifier circuit (Fig. 8*c*) to further control the amplitude of the error signal.

To obtain the third-derivative error signal, the standard saturated absorption setup is replaced by our simplified version seen in Fig. 3*b*. Also, we send the third-harmonic signal of the modulation frequency to the lock in, instead of the modulation itself. To generate the third harmonic of the modulation frequency, we use a commercial RF frequency doubler, another RF mixer, and a custom built high-pass filter with a steep cutoff below 150 kHz, as shown in Fig. 9. The third-derivative error signal is obtained by using a mixer and a low-pass filter as described previously. However, the amplitude A of the frequency modulation may have to be increased to ensure that the third-derivative component of the absorption signal is significant over the modulation range.

Fig. 10. (*a*) Energy level diagram for ^{85}Rb. (*b*) Saturated absorption signal seen in absorption as the laser frequency is scanned over the $F = 3$ to $F' = 2$, 3, 4 transitions: The peaks corresponding to these transition are labeled by 2, 3, and 4, respectively. The tallest peaks labeled CO are cross-over resonances [5]. The spacing between the two cross-over peaks is 60.5 MHz.
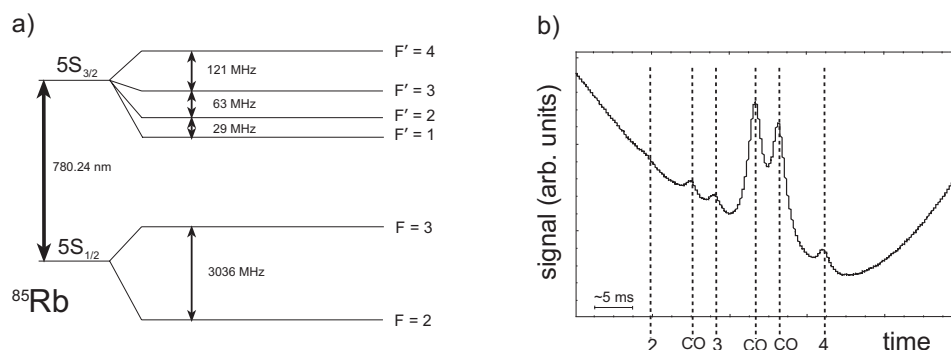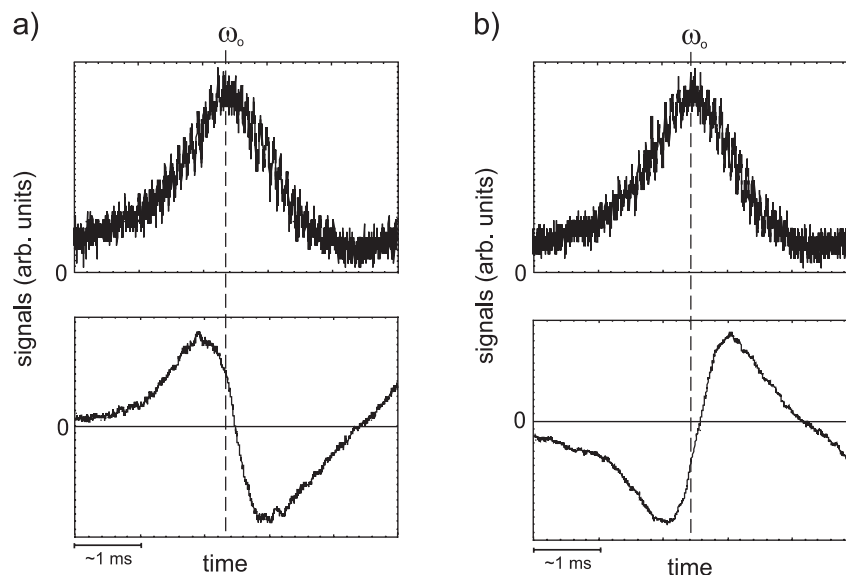

Fig. 11. Absorption signal showing a resonance peak at ω_0 and corresponding first derivative error signals: (*a*) $\phi = 0°$, (*b*) $\phi = 180°$. The shift in the zero crossing is the result of filtering the mixer output, which causes a time delay. Nevertheless, the laser is locked to the desired atomic resonance.


4. Results and discussion

Figure 10*a* shows the level structure of ^{85}Rb. Figure 10*b* shows the corresponding ^{85}Rb spectrum observed in absorption using the setup shown in Fig. 3*b*. We typically lock to a cross-over resonance because it has the largest amplitudes.

The first-derivative error signals at different values of ϕ are shown in Fig. 11. These signals were obtained by scanning the laser at $\sim$10 Hz. The error signals exhibit the shape and ϕ-dependence predicted in Sect. 2. The zero crossings of the error signals do not occur at ω_0 due to the filtering of the mixer output that is essential for obtaining the desired signal. This results in a time delay in correcting the laser frequency, thereby setting a minimum value for the overall time constant of the feedback loop.

Fig. 12. Absorption signal and corresponding third derivative error signal: The peaks are the two tallest cross-over resonances shown in Fig. 10*b*. The effect of the Doppler background is nearly eliminated. The shift in the zero crossing is a result of filtering the mixer output, which causes a time delay. Nevertheless, the laser is locked to the desired atomic resonance.
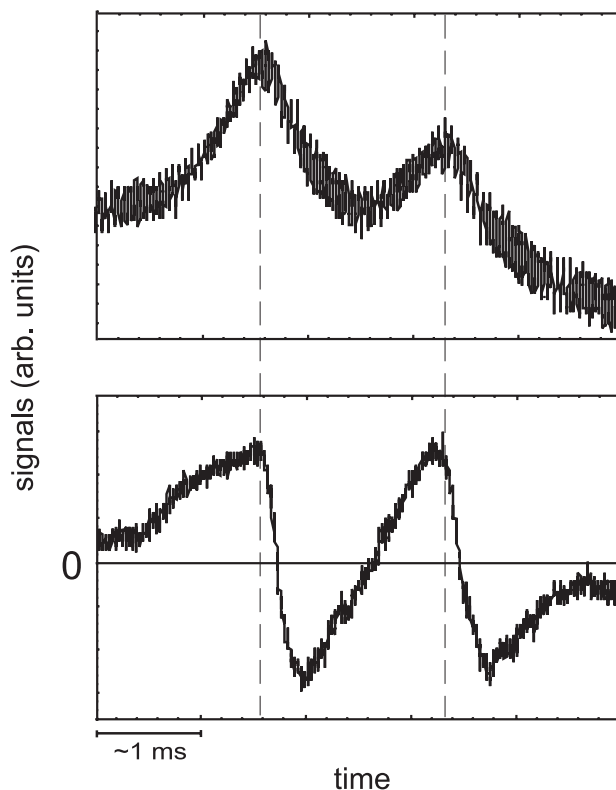

This time constant can be adjusted by changing the cutoff frequency of the low-pass filter in Fig. 8*b*.

Figure 12 shows the cross-over peaks and the corresponding third-derivative error signal. We checked that it was the third derivative by changing the phase of the modulation Ω (see input of Fig. 9) by π and verifying that the error signal changed sign three times. This test was performed because the frequency of the mixing signal at 3Ω contained a small component at Ω, which could result in the first derivative after mixing. We note that if we had been observing the first derivative, the signal would have changed sign only once.

Figure 13 shows the third-derivative error signal with and without engaging the feedback loop. It was recorded with the laser frequency initially centered on resonance and the scan turned off. From the known values of the Rb level splitting, it was possible to estimate the frequency excursions of the locked laser to be less than 1 MHz from the amplitude fluctuations of the error signal.

To further observe the effectiveness of the error signals, the feedback loop was engaged and the fluorescence from a laser-cooled sample of Rb atoms was monitored. For both the first- and third-derivative error signals, the fluctuations in the fluorescence (proportional to the number of trapped atoms) were limited to 2% for time scales of ∼1 h. Similar results were obtained with a commercial lock-in. As a comparison, with lock disengaged, the trap fluorescence typically drops by 10% in about 1 min.

The lock-in method of frequency stabilization necessarily involves modulating the resonance peak from which the error signal is generated. An advantage of this so-called modulation spectroscopy is the

Fig. 13. Third-derivative error signal with and without engaging the feedback loop.
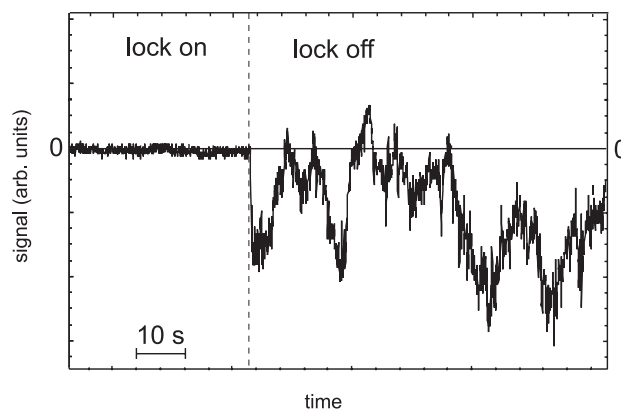
high signal-to-noise ratio obtained for the error signal. Any noise components not at the modulation frequency are eliminated in the mixing and filtering stage of the lock-in process. Although filtering the mixer output lowers the reaction time of the feedback loop, the modulation frequency can be increased to avoid this problem. We note that the modulation frequency is limited only by the response time of the atomic system (typically a few nanoseconds in atomic vapors). However, our choice of the modulation frequency (50 kHz) was dictated by the response time of the analog phase shifter and RF oscillator used to drive the AOM.

It is interesting to note that all-optical methods of frequency stabilization, that do not require modulating the signal, have been developed. Such methods include polarization spectroscopy [8] and the dichroic atomic-vapor laser lock [9] that make use of optically or magnetically induced dichroism, respectively, to produce dispersion shapes to be used as feedback.

We have been able to demonstrate a simple all-optical scheme that uses the side of the Doppler-broadened absorption as feedback. A DC offset was electronically added to the signal such that it crossed zero near the region of maximum slope. This results in an error signal with a very large recapture range and time delay determined by the atomic frequency response. Additionally, this method is less expensive and easier to set up than the other all-optical methods mentioned above. However, the error signal is strongly affected by intensity fluctuations. One method of stabilizing the error signal is to electronically divide it by the output of a reference photo detector that directly monitors the laser power.

A similar scheme, demonstrated in ref. 10, is called fringe-side (or tilt) locking. It also employs a reference photo detector for monitoring the laser power. In this case, a stable zero crossing is created by subtracting the output of the reference detector from the absorption signal.

5. Conclusions

We have developed a relatively inexpensive and versatile lock-in that can be used to stabilize the laser frequency for atom trapping applications. The overall cost of the components of the lock-in for obtaining the first-derivative error signal is under $200. For obtaining the third-derivative signal, the additional expenses incurred were ∼$500. This makes it feasible to adapt the experiment in advanced undergraduate laboratories to explain the principles of lock-in spectroscopy.

Acknowledgements

References

1. W. Demtroder. Laser spectroscopy: Basic concepts and instrumentation. Springer Verlag, New York. 1981.
2. H. Wahlquist. J. Chem. Phys. **35**, 1708 (1961).
3. R.L. Smith. JOSA, **61**, 8 (1971).
4. M. Weel and A. Kumarakrishnan. Can. J. Phys. **80**, 1449 (2002).
5. M.D. Levenson. Introduction to nonlinear laser spectroscopy. Boston Academic Press, Boston, USA. 1988.
6. C.C. Davis. Lasers and electro-optics. Cambridge University Press, Cambridge. 1996.
7. G. Spirou, I. Yavin, M. Weel, A. Vorozcovs, A. Kumarakrishnan, P.R. Battle, and R.C. Swanson. Can. J. Phys. **81**, 625 (2003).
8. R.J. Forster and N. Langford. JOSA B, **14**, 2083 (1997).
9. K.L. Corwin, Z. Lu, C.F. Hand, R.J. Epstein, and C.E. Wieman. Appl. Opt. **37**, 3295 (1998).
10. M. Marano, P. Laporta, A. Sapia, and P. De Natale. Opt. Lett. **25**, 1702 (2000).